*Inorg. Chem.* **2005**, *44*, 1230–1237


# Synthesis and Characterization of a Porous Magnetic Diamond Framework, $Co_3(HCOO)_6$, and Its $N_2$ Sorption Characteristic

**Zheming Wang,*[,†,‡] Bin Zhang,[†,§] Mohamedally Kurmoo,[∥] Mark A. Green,[⊥] Hideki Fujiwara,[†] Takeo Otsuka,[†] and Hayao Kobayashi*[,†]**

*Institute for Molecular Science and CREST, Japan, Science and Technology Coorporation, Okazaki 444-8585, Japan, College of Chemistry and Molecular Engineering, Peking University, Beijing 100871, China, Institute of Chemistry, Chinese Academy of Sciences, Beijing 100080, China, Laboratoire de Chimie de Coordination Organique, UMR7140-CNRS, Université Louis Pasteur, Institut Le Bel, 4 rue Blaise Pascal, 67000 Strasbourg Cedex, France, Royal Institution of Great Britain, 21 Albemarle Street, London W1X 4BS, U.K., and Department of Chemistry, University College of London, 20 Gordon Street, London WC1H OAJ, U.K.*

Received July 27, 2004

$[Co_3(HCOO)_6](CH_3OH)(H_2O)$ (**1**), the isostructural analogue of the porous magnet of coordination framework $[Mn_3(HCOO)_6](CH_3OH)(H_2O)$, and its desolvated form $[Co_3(HCOO)_6]$ (**2**) were prepared and characterized by X-ray and neutron diffraction methods, IR, thermal analyses, and BET, and their magnetic properties were measured. The parent compound, **1**, crystallizes in the monoclinic system, space group $P2_1/c$, $a = 11.254(2)$ Å, $b = 9.832(1)$ Å, $c = 18.108(3)$ Å, $\beta = 127.222(2)°$, $V = 1595.5(4)$ Å$^3$, $Z = 4$, R1 = 0.0329 at 180 K. It possesses a unit cell volume that is 9% smaller than $[Mn_3(HCOO)_6](CH_3OH)(H_2O)$ due to the smaller radius of $Co^{2+}$ ion. Compared with the parent compound **1**, the desolvated compound **2** has slightly larger lattice with cell parameters of $a = 11.2858(4)$ Å, $b = 9.8690(4)$ Å, $c = 18.1797(6)$ Å, $\beta = 127.193(2)°$, $V = 1613.0(1)$ Å$^3$, R1 = 0.0356 at 180 K. The cell parameters of **2**, obtained from neutron powder data at 2 K, are $a = 11.309(2)$ Å, $b = 9.869(1)$ Å, $c = 18.201(3)$ Å, $\beta = 127.244(8)°$, $V = 1617.3(5)$ Å$^3$. The pore volume reduces from 33% to 30% by replacing Mn by Co. The material exhibits a diamond framework based on Co-centered $CoCo_4$ tetrahedral nodes, in which all metal ions have octahedral coordination geometry and all HCOO groups link the metal ions in *syn–syn*/*anti* modes. It displays thermal stability up to 270 °C. The compound easily loses guest molecules without loss of crystallinity, and it partly reabsorbs water from the atmosphere. Significant $N_2$ sorption was observed for the desolvated framework suggesting that the material possesses permanent porosity. The magnetic properties show a tendency to a 3D long-range magnetic ordering, probably antiferromagnetic with a spin canting arrangement below 2 K.

## Introduction

Materials possessing two or more functionalities have caught much attention recently due to the possibility of producing materials where one property can be modified by tuning the other.[1−8] Over the past few years, our principal interest has focused on combining electrical conductivity with magnetism in molecule-based solids, and as such, we have

* To whom correspondence should be addressed. E-mail: hayao@ims.ac.jp (H.K.); zmw@pku.edu.cn; (Z.W.). Phone and fax: 81(Japan)-564-54-2254 (H.K.). Phone: 8610(China)-62755926 (Z.W.). Fax: 8610(China)-62751708 (Z.W.).

† Institute for Molecular Science and CREST, Japan, Science and Technology Coorporation.

‡ Peking University.

§ Chinese Academy of Sciences. E-mail: zhangbin@iccas.ac.cn.

∥ Université Louis Pasteur, Institut Le Bel. E-mail: kurmoo@chimie.u-strasbg.fr.

⊥ Royal Institution of Great Britain and University College of London. E-mail: mark@ri.ac.uk.

(1) (a) Coronado, E.; Galan-Máscarós, J. R.; Gómez-García, C. J.; Laukhin, V. *Nature* **2000**, *408*, 447. (b) Alberola, A.; Coronado, E.; Gálan-Máscarós, J. R.; Giménez-Saiz, C.; Gómez-García, C. J. *J. Am. Chem. Soc.* **2003**, *125*, 10774.

(2) (a) Rashid, S.; Turner, S. S.; Day, P.; Light, M. E.; Hursthouse, M. B.; Firth, S.; Clark, R. J. H. *Chem. Commun.* **2001**, 1462. (b) Clément, R.; Decurtins, S.; Gruselle, M.; Train, C. *Monatsh. Chem.* **2003**, *134*, 117.

(3) Kurmoo, M.; Graham, A. W.; Day, P.; Coles, S. J.; Hursthouse, M. B.; Caulfield, J. L.; Singleton, J.; Pratt, F. L.; Hayes, W.; Ducasse, L.; Guioneeau, P. *J. Am. Chem. Soc.* **1995**, *117*, 12209.

(4) (a) Tanaka, H.; Kobayashi, H.; Kobayashi, A.; Cassoux, P. *Adv. Mater.* **2000**, *12*, 1685. (b) Fujiwara, E.; Fujiwara, H.; Kobayashi, H.; Otsuka, T.; Kobayashi, A. *Adv. Mater*. **2002**, *14*, 1376.



10.1021/ic048986r CCC: $30.25 
Published on Web 02/15/2005

put in evidence the presence of (a) superconductivity and paramagnetism,[3] (b) superconductivity and long-range antiferromagnetic ordering,[4] and (c) field-induced reconstruction of Fermi surface and suppression of metal−insulator transition in favor of superconductivity,[5] in hybrids containing tetrathiafulvalene derivatives with transition metal complex anions. While others have most recently been interested in combining optical and magnetic properties,[6,7] we have embarked on the search for molecular systems combining magnetism with a structural aspect such as porosity.[8]

The synthesis of porous coordination materials in the recent years has been associated with the hydro- or solvothermal technique for historical reasons, following the work on silicate and phosphate zeolites.[9] Robl was one of the first to use the technique of solution chemistry by diffusion in gels to produce porous coordination polymers containing polycarboxylates.[10] Yaghi et al.[11] have developed a strategy, based on the concept of secondary building unit (SBU), and have successfully shown that one can enlarge the pore size by extending the bridging dicarboxylates. The large SBU nodes prohibit the interpenetration thus resulting in the nanoporosity. Kitagawa et al.[12] have employed a different strategy, that of the "pillared-layer" idea, to construct porous frameworks rationally. The simple modification of organic pillars can modulate not only the size of the nanospace but also the chemical functionality. Other approaches using bulky ligands or linear coordination polymer have also been applied.[13] However, it is now well understood that predesigning a building block, in situ or ex situ, is not a strict requirement. In many cases, the right choice of the metal centers, the ligand, and the counterion or the templating molecule is the most important factor, and serendipity is usually the prevailing state of things rather than the rule.

Porous coordination frameworks have several advantages,[11−14] which have been realized and taken up by several groups, over their inorganic analogues, i.e., zeolites. The infinite richness in the arrangement, size, property, and modification of the nanoscale space of coordination framework and the high stability and flexibility for guest-insertion, guest-removal, or exchange open up a whole gamut of possible structures, functionalities, and applications. The most important advantage is, due to the coordination frameworks possessing magneto-, electro-, or photoactive metal ions, interactions (electronic, magnetic, photonic, etc.) within the framework as well as between the guest and the host framework, which give further functionalities. Therefore, porous coordination materials, in addition to the porosity, provide a new approach to explore multifunctionalities.[14]

In this context, porous magnets are of special interest because the possibility to modulate magnetic properties upon guest exchange renders them attractive for applications as devices and sensors.[15−17] It should be pointed out that the synthesis of porous magnets remains a challenge since long-range magnetic ordering and porosity are inimical to one another.[16] Reported porous magnets include metal−organic radical complexes,[17] pillared layered metal−hydroxide materials,[8] organic−inorganic hybrid materials with metal oxide frameworks,[18] and Prussian blue,[19] but examples are still few until now. Especially, those with permanent porosity are very rare. We have recently shown that it is possible to synthesize a magnetic porous framework of $Mn_3(HCOO)_6$ by using solution chemistry.[16] Kim et al. also prepared this framework compound using a solvothermal process.[20] From the point of view of coordination chemistry, it is important to note that the compound is built with the smallest of the carboxylates contrary to the use of extended ligands as is commonly believed to be the basic requirement for obtaining porous materials. From a structural point of view, the framework is based on a diamond network (thus its stability) of octahedrally coordinated divalent metals, and the thick metal−formate walls result in the presence of the porous channels. As expected, the compound is fairly stable due to the strong coordination bonds and as mentioned above to its diamond structure. We also demonstrated that the framework shows


(5) (a) Fujiwara, H.; Kobayashi, H.; Fujuwara, E.; Kobayashi, A. *J. Am. Chem. Soc.* **2002**, *124*, 6816. (b) Zhang, B.; Tanaka, H.; Fujiwara, H.; Kobayashi, H.; Fujiwara, E.; Kobayashi, A. *J. Am. Chem. Soc.* **2002**, *124*, 9982. (c) Uji, S.; Shinagawa, H.; Terashima, T.; Yakabe, T.; Terai, Y.; Tokumoto, M.; Kobayashi, A.; Tanaka, H.; Kobayashi, H. *Nature* **2001**, *410*, 908.

(6) (a) Sato, O. *Acc. Chem. Res.* **2003**, *36*, 692. (b) Sunatsuki, Y.; Ikuta, Y.; Matsumoto, N.; Ohta, H.; Kojima, M.; Iijima, S.; Hayami, S.; Maeda, Y.; Kaizaki, S.; Dahan, F.; Tuchagues, J. P. *Angew. Chem., Int. Ed.* **2003**, *42*, 1614.

(7) (a) Lacroix, P. G.; Malfant, I.; Bénard, S.; Yu, P.; Rivière, E.; Nakatani, K. *Chem. Mater.* **2001**, *13*, 441. (b) Barron, L. D.; Buckingham, A. D. *Acc. Chem. Res.* **2001**, *34*, 781. (c) Inoue, K.; Kikuchi, K.; Ohba, M.; Ōkawa, H. *Angew. Chem., Int. Ed.* **2003**, *42*, 4810.

(8) (a) Rujiwatra, A.; Kepert, C. J.; Claridge, J. B.; Rosseinsky, M. J.; Kumagai, H.; Kurmoo, M. *J. Am. Chem. Soc.* **2001**, *123*, 10584. (b) Kurmoo, M.; Kumagai, H.; Hughes, S. M.; Kepert, C. J. *Inorg. Chem.* **2003**, *42*, 6709.

(9) (a) Thomas, J. M.; Thomas, W. J. *Princ. Pract. Heterogen. Catal.* **2003**, *216*, 298 and references therein. (b) Cundy, C. S.; Cox, P. A. *Chem. Rev.* **2003**, *103*, 663. (c) Corma, A. *J. Catal.* **2003**, *216*, 298.

(10) Robl, C. *Z. Anorg. Allg. Chem.* **1987**, *554*, 79.

(11) (a) Yaghi, O. M.; O'Keeffe, M.; Ockwig, N. W.; Chae, H. K.; Eddaoudi, M.; Kim, J. *Nature* **2003**, *423*, 705 and references cited therein. (b) Eddaoudi, M.; Kim, J.; Rosi, N.; Vodak, D.; Wachter, J.; O'Keeffe, M.; Yaghi, O. *Science* **2002**, *295*, 469. (c) Eddaoudi, M.; Moler, D. B.; Li, H.-L.; Chen, B.-L.; Reineke, T. M.; O'Keeffe, M.; Yaghi, O. M. *Acc. Chem. Rev.* **2001**, *34*, 319. (d) Forster, P. M.; Cheetham, A. K. *Top. Catal.* **2003**, *24*, 79. (d) Cheetham, A. K.; Férey, G.; Loiseau, T. *Angew. Chem., Int. Ed.* **1999**, *38*, 3268. (e) Harrison, W. T. A. *Curr. Opin. Solid State Mater.* **2002**, *6*, 407.

(12) (a) Maji, T. K.; Uemura, K.; Chang, H.-C.; Matsuda, R.; Kitagawa, S. *Angew. Chem., Int. Ed.* **2004**, *43*, 3269. (b) Kitagawa, S.; Kitaura, R. *Comments Inorg. Chem.* **2002**, *23*, 101. (c) Kitaura, R.; Fujimoto, K.; Noro, S.; Kondo, M.; Kitagawa, S. *Angew. Chem., Int. Ed.* **2002**, *41*, 133. (d) Kondo, M.; Okubo, T.; Asami, A.; Noro, S.; Yoshitomi, T.; Kitagawa. S.; Ishii, T.; Matsuzaka, H.; Seki, K. *Angew. Chem., Int. Ed.* **1999**, *38*, 140.

(13) (a) Xu, X.; Nieuwenhuyzen, M.; James, S. L. *Angew. Chem., Int. Ed.* **2002**, *41*, 764. (b) Lee, E. Y.; Suh, M. P. *Angew. Chem., Int. Ed.* **2004**, *43*, 2798.

(14) (a) Kitagawa, S.; Kitaura, R.; Noro, S. *Angew. Chem., Int. Ed.* **2004**, *43*, 2334. (b) Rao, C. N. R.; Natarajan, S.; Vaidhyanathan, R. *Angew. Chem., Int. Ed.*, **2004**, *43*, 1466.

(15) Halder, G. J.; Kepert, C. J.; Moubaraki, B.; Murray, K. S.; Cashion, J. D. *Science* **2002**, *298*, 1762.

(16) Wang, Z.-M.; Zhang, B.; Fujiwara, H.; Kobayashi, H.; Kurmoo, M. *Chem. Commun.* **2004**, 416.

(17) Maspoch, D.; Ruiz-Molina, D.; Wurst, K.; Domingo, N.; Cavallini, M.; Biscarini, F.; Tejada, J.; Rovira, C.; Veciana, J. *Nat. Mater.* **2003**, *2*, 190.

(18) (a) Guillou, N.; Livage, C.; Drillon, M.; Férey, G. *Angew. Chem., Int. Ed.* **2003**, *42*, 5314. (b) Guillou, N.; Livage, C.; van Beek, W.; Noguès, M.; Férey, G. *Angew. Chem., Int. Ed.* **2003**, *42*, 643.

(19) Beauvais, L. G.; Long, J. R. *J. Am. Chem. Soc.* **2002**, *124*, 12096.

(20) Dybtsev, D. N.; Chun, H.; Yoon, S. H.; Kim, D.; Kim, K. *J. Am. Chem. Soc.* **2004**, *126*, 32.

high stability and flexibility for the inclusion of many kinds of guests,[16,20] and the occluded molecules can be gas and liquid as well as solid, including tetrathiafulvalene, in their pure state, where the latter two were inserted from their vapors. The framework exhibits ferrimagnetic ordering with guest-modulated critical temperature.[16] This success prompted us to look for analogues with other divalent first-row transition metals.[21] Our motives are twofold: (a) to control the pore size by using divalent cations having different radii (for example: Mn (0.95Å), Co (0.80Å), and Ni (0.74Å)), and (b) to study the magnetic interactions by changing the electronic configuration as well as introducing magnetic anisotropy in the system. We report here the successful synthesis of the cobalt analogue $[Co_3(HCOO)_6](CH_3OH)(H_2O)$ (**1**) and its desolvated form $Co_3(HCOO)_6$ (**2**). It is of much interest for its framework topology, the permanent porosity, thermal stability, significant $N_2$ sorption behavior, and a tendency to 3D long-range magnetic ordering.

## Experimental Section

**Preparation of 1 and 2.** A small vessel containing a solution of $CoCl_2 \cdot 6H_2O$ (0.72 g) in methanol (10 mL) was placed in a large vessel containing a mixture of triethylamine (1.34 g) and formic acid (0.92 g) in methanol (25 mL). Methanol (15 mL) was then carefully layered onto the two solutions until they shared a common layer of methanol that acts as a pathway for slow diffusion. Small red thin plate crystals appeared after 4 or 5 days. Crystallization took one month and gave crystals in a yield of 90% based on cobalt salt. The crystals lose solvent molecules slowly in air at room temperature without degradation. The crystals were found to be heavily twinned. Anal. Calcd for **1**, $C_7H_{12}O_{14}Co_3$: C, 16.92, H, 2.43%. Found: C 17.42, H, 2.36%. IR bands ($cm^{-1}$) for **1**: 3100−3600br, 2928w, 2893w, 1722w, 1588vs, 1392m, 1333s, 1210w, 1163w, 1060w, 790m.

The desolvated form, **2**, was obtained by pumping on the sample of **1** while heating at ca. 90 °C. The desolvation procedure lasted overnight, which resulted in a weight loss of 9.6% upon guest removal. Anal. Calcd for **2**, $C_6H_6O_{12}Co_3$: C, 16.13, H, 1.35%. Found: C, 15.45, H, 2.02%. IR bands ($cm^{-1}$) for **2**: 2894w, 1590vs, 1388m, 1336s, 790m.

**Crystallography Study.** Because of the heavy twinning habit of the thin plate crystals of both **1** and **2**, we had great difficulty in obtaining suitable single crystals. During the diffraction experiments, the small pieces of crystals of **1** or **2**, carefully cut from large twins, were checked carefully until the diffraction patterns revealed that the checked crystals were suitable for further diffraction experiments. The crystallographic data were collected at 87 and 180 K on a Rigaku AFC7 Mercury CCD diffractometer with 5.4 kW rotating anode source for **1**,[22a] and at 105 and 180 K on a Nonius KappaCCD diffractometer with 2.0 kW sealed tube source for **2**,[22b,c] both using graphite monochromated Mo Kα radiation of $\lambda = 0.71073$ Å. The structures were solved by direct methods, and refined by full-matrix least-squares on $F^2$ using SHELX program.[23] The H atoms of the framework, i.e., H atoms of HCOO groups, were located from the difference Fourier synthesis and refined isotropically. The refined C−H distances, bond angles involving H atoms, and isotropic thermal factors of H atoms are all of rational values. The severely disordered solvent molecules, one $CH_3OH$ and one water per formula in **1**, were modeled in two and three locations, respectively, and without addition of the H atoms. The structure of **2**, however, showed empty channels, as indicated by the low final residual electron densities in the channels. The details of data collection, data reduction, and crystallographic data at 180 K are summarized in Table 1, together with the crystallography data of the Mn analogues,[16] $[Mn_3(HCOO)_6](CH_3OH)(H_2O)$ (**3**) and $[Mn_3(HCOO)_6]$ (**4**), both at 180 K, for comparison.

Powder XRD patterns for **1**, **2**, and the samples of **2** after the gas adsorption experiment (BET) were obtained on a Rigaku RINT2000 diffractometer at room temperature with Cu Kα radiation in a flat plate geometry.

Neutron diffraction of the desolvated compound, **2**, was performed on the D20 powder diffractometer at the Institut Laue Langevin, Grenoble, as a function of temperature down to 2 K and using a wavelength of 2.419 Å. Data were analyzed by the GSAS suite of programs,[24] using the atomic coordinates and unit cell parameters of **1** of 87 K as the starting structure model.

**Physical Measurements.** FTIR spectra were recorded using pure sample of **1** and **2** in the range 4000− 650 $cm^{-1}$ on a Nicolet Magna 750 FT/IR spectrometer. dc magnetic data of **1** were obtained on a Quantum Design MPMS7EB SQUID system and of **2** on an MPMS5XL SQUID system, and ac data of **1** were obtained on an Oxford MagLab2000 system. Diamagnetic corrections were estimated using Pascal constants[25] ($-173 \times 10^{-6}$ and $-138 \times 10^{-6}$ $cm^3\ mol^{-1}$ for **1** and **2**, respectively), and background correction was estimated by experimental measurement on sample holders. Thermal analyses, TGA, DTA, and DSC, were performed on a Hi-Res TGA 2950 thermogravimetric analyzer, a SDT 2960 thermal analyzer, and a DSC 2010 differential scanning calorimeter, respectively, at 10 °C/min under $N_2$. The $N_2$ sorption experiment was carried out on an adsorption apparatus of ASAP 2010 Micromeritics at 77.4 K.

## Results and Discussion

**Synthesis.** The two porous compounds $[M_3(HCOO)_6](CH_3OH)(H_2O)$ (M = Co, **1**, Mn, **3**) [21] were prepared by the reaction of divalent metal chlorides with formic acid neutralized by triethylamine in methanol. This method also works when the triethylamine is replaced by other bulky amines such as diethylamine or propylamine. However, the use of smaller amines results in the perovskite compounds, $[AmineH^+][M(HCOO)_3]$, with a NaCl-like anionic framework incorporating the cationic ammonium within the cubic cavities.[26] From a series of experiments using many different

(21) We have very recently obtained the Fe(II) and Zn(II) analogues, the other two members of the family. Both are isostructural to the Co and Mn compounds reported here. The lattice parameters at 180 K are the following: for the Fe analogue, $a = 11.367$ Å, $b = 9.892$ Å, $c = 18.239$ Å, $\beta = 127.259°$, $V = 1632.3$ Å$^3$; for the Zn analogue, $a = 11.240$ Å, $b = 9.782$ Å, $c = 18.058$ Å, $\beta = 127.107°$, $V = 1583.4$ Å$^3$.

(22) (a) *CrystalClear* software; Rigaku Corp.: Japan, 2000. (b) *Collect* data collection software; Nonius BV: Delft, The Netherlands, 1998. (c) *HKL2000* and *maXus* software; University of Glasgow: Scotland, U.K.; Nonius BV: Delft, The Netherlands; MacScience Co. Ltd.: Yokohama, Japan, 2000.

(23) Sheldrick, G. M. *SHELX-97, Program for Crystal Structure Determination*; University of Göttingen: Göttingen, Germany, 1997.

(24) Larson, A. C.; von Dreele, R. B. *General Structure Analysis System (GSAS)*; Los Alamos Laboratories Report LAUR 86-748; Los Alamos, NM, 2000.

(25) Mulay, L. N.; Boudreaux, E. A. *Theory and Applications of Molecular Diamagnetism*; John Wiley & Sons Inc.: New York, 1976.

(26) (a) Wang, Z.-M.; Zhang, B.; Otsuka, T.; Inoue, K.; Kobayashi, H.; Kurmoo, M. *Dalton Trans*. **2004**, 2209. (b) Wang, X.-Y.; Gan, L.; Zhang, S.-W.; Gao, S. *Inorg. Chem.* **2004**, *43*, 4615.

**Table 1.** Crystallographic Data for Compounds **1**−**4**

| | **1** | **2** | **3**[a] | **4**[b] |
|---|---|---|---|---|
| formula | $C_7H_{12}Co_3O_{14}$ | $C_6H_6Co_3O_{12}$ | $C_7H_{12}Mn_3O_{14}$ | $C_6H_6Mn_3O_{12}$ |
| fw | 496.96 | 446.90 | 484.99 | 434.93 |
| $T$, K | 180 | 180 | 180 | 180 |
| cryst syst | monoclinic | monoclinic | monoclinic | monoclinic |
| space group | $P2_1/c$ | $P2_1/c$ | $P2_1/c$ | $P2_1/c$ |
| $a$, Å | 11.254(2) | 11.2858(4) | 11.650(1) | 11.729(1) |
| $b$, Å | 9.832(1) | 9.8690(4) | 10.128(1) | 10.192(1) |
| $c$, Å | 18.108(3) | 18.1797(6) | 18.614(2) | 18.742(2) |
| α, deg | 90 | 90 | 90 | 90 |
| $\beta$, deg | 127.222(2) | 127.193(2) | 127.056(3) | 127.178(3) |
| $\gamma$, deg | 90 | 90 | 90 | 90 |
| $V$, Å$^3$ | 1595.5(4) | 1613.0(1) | 1752.6(3) | 1785.2(3) |
| $Z$ | 4 | 4 | 4 | 4 |
| $D_c$, g/cm$^3$ | 2.069 | 1.840 | 1.838 | 1.618 |
| $\mu$(Mo $K\alpha$), mm$^{-1}$ | 3.152 | 3.098 | 2.192 | 2.134 |
| cryst size, mm$^3$ | 0.09 × 0.07 × 0.05 | 0.15 × 0.12 × 0.05 | 0.16 × 0.14 × 0.14 | 0.12 × 0.11 × 0.09 |
| $T_{max}$ and $T_{min}$ | 0.879, 1.000 | 0.704, 0.860 | 0.862, 1.000 | 0.868, 1.000 |
| $\theta_{min}$, $\theta_{max}$, deg | 3.08, 27.48 | 3.49, 27.47 | 3.02, 27.48 | 3.00, 27.48 |
| no. total reflns | 27214 | 28990 | 28835 | 29323 |
| no. unique reflns ($R_{int}$) | 3621 (0.0507) | 3688 (0.114) | 3950 (0.0414) | 4068 (0.0672) |
| no of obsd reflns [$I \geq 2\sigma(I)$] | 2915 | 2583 | 3251 | 3043 |
| no. params | 246 | 218 | 245 | 218 |
| R1,wR2 [$I \geq 2\sigma(I)$] | 0.0329, 0.0763 | 0.0356, 0.0750 | 0.0305, 0.0811 | 0.0302, 0.0581 |
| R1,wR2 (all data) | 0.0492, 0.0799 | 0.0645, 0.0807 | 0.0413, 0.0836 | 0.0546, 0.0622 |
| GOF | 1.086 | 0.981 | 1.101 | 0.963 |
| $\Delta\rho$,[c] e/Å$^3$ | 0.469, −0.523 | 0.455, −0.591 | 0.657, −0.345 | 0.376, −0.334 |
| Max and mean $\Delta/\sigma$[d] | 0.001, 0.000 | 0.000, 0.000 | 0.001, 0.000 | 0.001, 0.000 |

[a] CCDC-210639. [b] CCDC-210640. [c] Max and min residual density. [d] Max and mean shift/esd.

amines, it is now clear that the use of large amines such as triethylamine and the use of noncoordinating solvent such as methanol are the two key requirements for producing the diamond framework compounds. Although absent in the final frameworks, the large protonated amine cations appear to be important for the formation of the porous framework. At least, the large size of the protonated amine cations inhibits the formation of anionic frameworks which were observed for the small cations.[26a] On the other hand, the use of noncoordinating solvent avoids the formation of metal−formates with co-ligands, as what was observed for many known metal−formates.[27] The synthesis of the nickel analogue has so far resulted in powders that have not been characterized yet. It is also to be noted that the crystal quality is better and size larger for the manganese compound than for the cobalt compound. The crystal quality becoming poorer for smaller metal ions and the difficulty in synthesizing the crystals of nickel compound were also observed for the [AmineH$^+$][M(HCOO)$_3$] of the M = Mn, Co, and Ni series[26a] where Ni compounds usually are powders or microcrystals.

**Structure of 1 and 2.** The selected molecular geometry of **1** and **2** is given in Table 2, together with that of **3** and **4**, which has not been provided in detail in the previous communications.[16,20] Compound **1** has the same diamond framework as **3**, but the nodes here are Co-centered $CoCo_4$ tetrahedra (Figure 1). The tetrahedron has one central Co ion (Co1), four apical Co ions (Co2, Co3, Co4, and Co2A), and six edged HCOO groups which link the metal ions in *syn*−*syn*/*anti* mode.[28] These tetrahedral units, by sharing their metal apices, form the diamond framework in which all Co atoms possess octahedral coordination geometry, rarely observed in diamond networks.[29] The Co−O bond distances of 2.040−2.115 Å are shorter than the Mn−O ones of 2.105−2.233 Å in **3** and in good agreement with the difference of ionic radii between $Co^{2+}$ and $Mn^{2+}$ (Table 2). Consequently, a smaller lattice and shorter Co−Co distances are observed, compared to the Mn analogue.[16] The bond angles around Co sites are 77.9−100.1° for *cis* O−Co−O angles and 164.6−180.0° for *trans* O−Co−O angles, characterizing the distortion of the $CoO_6$ octahedra. Co−Co distances are Co1−Co2, 3.179 and 3.156 Å, Co1−Co3, 3.508 Å, Co1−Co4, 3.480 Å, apical Co−Co, 5.227−5.627 Å, and Co1−O−Co2 angles in pairs, 97.7° and 96.7°, and 99.6° and 97.5°, Co1−O−Co3 angle, 115.0°, Co1−O−Co4, 112.8°, respectively. In the structure, Co−Co linkages include short single-atom (Co−O−Co) and three-atom (Co−O−C−O−Co) bridges. Considering Co−O−Co connections, the structure can be considered as chains of edge-sharing Co1 and Co2 octahedra further connected by Co3 and Co4 octahedra via apex-sharing. In addition to coordination bonds, all HCOO ligands are involved in weak C−H···O H-bonds[30] with C···O distances of 2.914−3.642 Å and C−H···O angles of 107−150°. These concerted weak interactions in fact strengthen the framework further and thus contribute to the framework stability described subsequently.

(27) See, for example, refs 7−12 cited in ref 26a.

(28) Carrell, C. J.; Carrell, H. L.; Erlebacher, J.; Glusker, J. P. *J. Am. Chem. Soc.* **1988**, *110*, 8651.
(29) Batten, S. R.; Robson, R. *Angew. Chem., Int. Ed.* **1998**, *37*, 1460.
(30) Steiner, T. *Angew. Chem., Int. Ed.* **2002**, *41*, 48.

**Table 2.** Selected Bond Distances (Å) and Angles (deg) for **1**−**4** at 180 K[a]

| | 1 | 2 | 3 | 4 | | 1 | 2 | 3 | 4 |
|---|---|---|---|---|---|---|---|---|---|
| M(1)−O(1) | 2.086(2) | 2.090(2) | 2.196(1) | 2.202(2) | O(2)−M(2)−O(5)$^{\#1}$ | 93.17(8) | 93.13(8) | 96.31(6) | 95.30(6) |
| M(1)−O(3) | 2.084(2) | 2.078(2) | 2.197(2) | 2.204(1) | O(2)−M(2)−O(12)$^{\#1}$ | 93.26(9) | 93.43(9) | 98.18(7) | 98.55(6) |
| M(1)−O(5) | 2.117(2) | 2.117(2) | 2.195(2) | 2.206(1) | O(3)−M(2)−O(7) | 78.10(8) | 77.57(8) | 77.73(6) | 77.65(5) |
| M(1)−O(7) | 2.116(2) | 2.112(2) | 2.183(1) | 2.187(2) | O(3)−M(2)−O(1)$^{\#1}$ | 92.76(7) | 92.94(8) | 90.04(5) | 90.70(6) |
| M(1)−O(9) | 2.045(2) | 2.046(2) | 2.140(1) | 2.140(2) | O(3)−M(2)−O(5)$^{\#1}$ | 171.46(8) | 171.42(8) | 168.16(6) | 168.64(6) |
| M(1)−O(11) | 2.070(2) | 2.064(2) | 2.159(2) | 2.162(1) | O(3)−M(2)−O(12)$^{\#1}$ | 92.79(8) | 92.86(9) | 92.73(6) | 91.98(6) |
| M(2)−O(2) | 2.049(2) | 2.053(2) | 2.116(2) | 2.121(2) | O(7)−M(2)−O(1)$^{\#1}$ | 87.60(8) | 87.98(8) | 85.09(6) | 85.30(5) |
| M(2)−O(3) | 2.078(2) | 2.087(2) | 2.161(1) | 2.164(2) | O(7)−M(2)−O(5)$^{\#1}$ | 100.10(8) | 100.75(9) | 98.84(6) | 99.55(5) |
| M(2)−O(7) | 2.115(2) | 2.115(2) | 2.225(2) | 2.223(1) | O(7)−M(2)−O(12)$^{\#1}$ | 170.86(8) | 170.41(8) | 169.47(6) | 168.82(6) |
| M(2)−O(1)$^{\#1}$ | 2.105(2) | 2.103(2) | 2.222(2) | 2.221(2) | O(1)$^{\#1}$−M(2)−O(5)$^{\#1}$ | 78.79(7) | 78.56(8) | 78.33(5) | 78.06(5) |
| M(2)−O(5)$^{\#1}$ | 2.106(2) | 2.113(2) | 2.182(1) | 2.189(2) | O(1)$^{\#1}$−M(2)−O(12)$^{\#1}$ | 92.18(8) | 91.99(9) | 90.51(6) | 90.72(6) |
| M(2)−O(12)$^{\#1}$ | 2.040(2) | 2.041(2) | 2.124(2) | 2.124(1) | O(5)$^{\#1}$−M(2)−O(12)$^{\#1}$ | 88.81(8) | 88.63(9) | 89.60(6) | 89.81(6) |
| M(3)−O(4) | 2.093(2) | 2.085(2) | 2.166(2) | 2.163(2) | O(4)−M(3)−O(6) | 91.10(8) | 91.01(9) | 89.88(6) | 89.88(7) |
| M(3)−O(6) | 2.064(2) | 2.065(2) | 2.149(2) | 2.163(2) | O(4)−M(3)−O(9) | 95.39(8) | 95.01(8) | 95.37(6) | 95.04(6) |
| M(3)−O(9) | 2.115(2) | 2.122(2) | 2.205(1) | 2.206(1) | O(4)−M(3)−O(4)$^{\#2}$ | 180.00 | 180.00 | 180.00 | 180.00 |
| M(3)−O(4)$^{\#2}$ | 2.093(2) | 2.085(2) | 2.166(2) | 2.163(2) | O(4)−M(3)−O(6)$^{\#2}$ | 88.90(8) | 88.99(9) | 90.12(6) | 90.12(7) |
| M(3)−O(6)$^{\#2}$ | 2.064(2) | 2.065(2) | 2.149(2) | 2.163(2) | O(4)−M(3)−O(9)$^{\#2}$ | 84.61(8) | 84.99(8) | 84.63(6) | 84.96(6) |
| M(3)−O(9)$^{\#2}$ | 2.115(2) | 2.122(2) | 2.205(1) | 2.206(1) | O(6)−M(3)−O(9) | 91.95(8) | 91.79(8) | 91.48(6) | 91.14(5) |
| M(4)−O(8) | 2.072(2) | 2.077(2) | 2.152(2) | 2.151(2) | O(6)−M(3)−O(4)$^{\#2}$ | 88.90(8) | 88.99(9) | 90.12(6) | 90.12(7) |
| M(4)−O(10) | 2.071(2) | 2.070(2) | 2.151(2) | 2.153(2) | O(6)−M(3)−O(6)$^{\#2}$ | 180.00 | 180.00 | 180.00 | 180.00 |
| M(4)−O(11) | 2.108(2) | 2.114(2) | 2.211(2) | 2.208(1) | O(6)−M(3)−O(9)$^{\#2}$ | 88.05(8) | 88.21(8) | 88.52(6) | 88.86(5) |
| M(4)−O(8)$^{\#3}$ | 2.072(2) | 2.077(2) | 2.152(2) | 2.151(2) | O(9)−M(3)−O(4)$^{\#2}$ | 84.61(8) | 84.99(8) | 84.63(6) | 84.96(6) |
| M(4)−O(10)$^{\#3}$ | 2.071(2) | 2.070(2) | 2.151(2) | 2.153(2) | O(9)−M(3)−O(6)$^{\#2}$ | 88.05(8) | 88.21(8) | 88.52(6) | 88.86(5) |
| M(4)−O(11)$^{\#3}$ | 2.108(2) | 2.114(2) | 2.211(2) | 2.208(1) | O(9)−M(3)−O(9)$^{\#2}$ | 180.00 | 180.00 | 180.00 | 180.00 |
| O(1)−M(1)−O(3) | 87.15(8) | 87.39(8) | 85.78(6) | 85.53(5) | O(4)$^{\#2}$−M(3)−O(6)$^{\#2}$ | 91.10(8) | 91.01(9) | 89.88(6) | 89.88(7) |
| O(1)−M(1)−O(5) | 78.97(8) | 78.75(8) | 78.60(5) | 78.09(6) | O(4)$^{\#2}$−M(3)−O(9)$^{\#2}$ | 95.39(8) | 95.01(8) | 95.37(6) | 95.04(6) |
| O(1)−M(1)−O(7) | 88.01(8) | 88.24(8) | 86.83(5) | 87.22(6) | O(6)$^{\#2}$−M(3)−O(9)$^{\#2}$ | 91.95(8) | 91.79(8) | 91.48(6) | 91.14(5) |
| O(1)−M(1)−O(9) | 173.51(8) | 173.05(9) | 173.24(6) | 171.61(5) | O(8)−M(4)−O(10) | 90.95(9) | 90.50(9) | 90.58(7) | 89.10(7) |
| O(1)−M(1)−O(11) | 88.77(8) | 88.84(8) | 88.93(6) | 89.11(6) | O(8)−M(4)−O(11) | 93.67(8) | 93.52(8) | 93.20(6) | 92.96(6) |
| O(3)−M(1)−O(5) | 93.05(7) | 93.19(8) | 92.14(6) | 92.54(5) | O(8)−M(4)−O(8)$^{\#3}$ | 180.00 | 180.00 | 180.00 | 180.00 |
| O(3)−M(1)−O(7) | 77.94(7) | 77.83(8) | 77.86(6) | 77.57(5) | O(8)−M(4)−O(10)$^{\#3}$ | 89.05(9) | 89.50(9) | 89.42(7) | 90.90(7) |
| O(3)−M(1)−O(9) | 89.96(8) | 89.75(8) | 89.65(6) | 89.27(5) | O(8)−M(4)−O(11)$^{\#3}$ | 86.33(8) | 86.48(8) | 86.80(6) | 87.04(6) |
| O(3)−M(1)−O(11) | 172.44(8) | 172.71(8) | 172.07(5) | 171.82(6) | O(10)−M(4)−O(11) | 92.44(8) | 92.07(8) | 92.15(6) | 91.31(5) |
| O(5)−M(1)−O(7) | 164.58(7) | 164.58(8) | 162.94(5) | 162.95(6) | O(10)−M(4)−O(8)$^{\#3}$ | 89.05(9) | 89.50(9) | 89.42(7) | 90.90(7) |
| O(5)−M(1)−O(9) | 95.39(8) | 95.10(8) | 96.63(5) | 95.60(6) | O(10)−M(4)−O(10)$^{\#3}$ | 180.00 | 180.00 | 180.00 | 180.00 |
| O(5)−M(1)−O(11) | 92.41(8) | 92.19(8) | 92.60(6) | 92.40(5) | O(10)−M(4)−O(11)$^{\#3}$ | 87.56(8) | 87.93(8) | 87.85(6) | 88.69(5) |
| O(7)−M(1)−O(9) | 97.08(8) | 97.35(8) | 97.08(6) | 98.10(6) | O(11)−M(4)−O(8)$^{\#3}$ | 86.33(8) | 86.48(8) | 86.80(6) | 87.04(6) |
| O(7)−M(1)−O(11) | 95.57(8) | 95.83(8) | 95.97(6) | 96.02(5) | O(11)−M(4)−O(10)$^{\#3}$ | 87.56(8) | 87.93(8) | 87.85(6) | 88.69(5) |
| O(9)−M(1)−O(11) | 94.72(8) | 94.67(8) | 96.11(6) | 96.73(6) | O(11)−M(4)−O(11)$^{\#3}$ | 180.00 | 180.00 | 180.00 | 180.00 |
| O(2)−M(2)−O(3) | 95.11(8) | 95.21(8) | 94.85(6) | 95.52(6) | O(8)$^{\#3}$−M(4)−O(10)$^{\#3}$ | 90.95(9) | 90.50(9) | 90.58(7) | 89.10(7) |
| O(2)−M(2)−O(7) | 88.32(8) | 88.07(8) | 87.20(6) | 86.74(6) | O(8)$^{\#3}$−M(4)−O(11)$^{\#3}$ | 93.67(8) | 93.52(8) | 93.20(6) | 92.96(6) |
| O(2)−M(2)−O(1)$^{\#1}$ | 170.20(8) | 169.97(9) | 169.80(7) | 168.63(6) | O(10)$^{\#3}$−M(4)−O(11)$^{\#3}$ | 92.44(8) | 92.07(8) | 92.15(6) | 91.31(5) |

[a] Symmetry codes: #1 $-x+1, y-1/2, -z+1/2$; #2 $-x+1, -y, -z$; #3 $-x, -y, -z$.

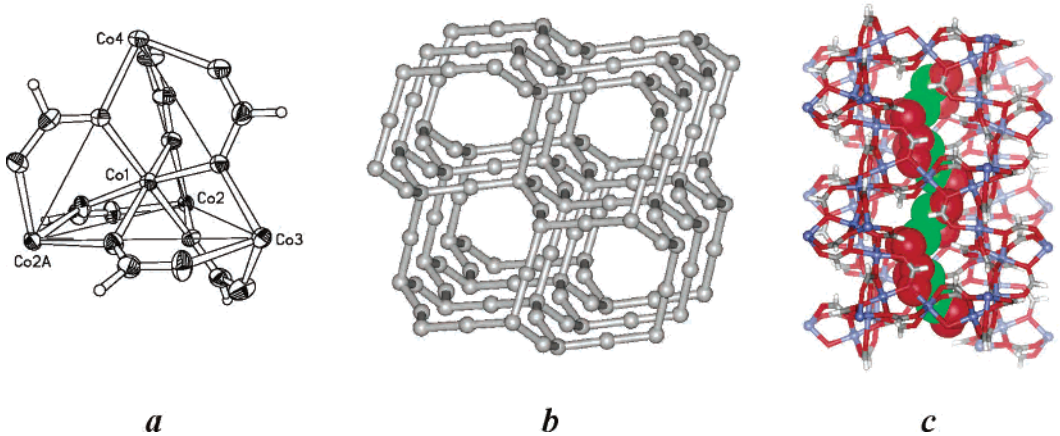


*a* *b* *c*

**Figure 1.** The structure of **1**: (a) the Co-centered $CoCo_4$ tetrahedron; (b) the porous diamond framework formed by the tetrahedral units as nodes sharing apices and showing open channels; (c) one channel with occupied and severely disordered guest molecules (one methanol and one water per formula), showing the zigzag character of the channel.

The open framework has channels running along the *b*-direction. The entrance of the channel is about 4 Å × 5 Å wide with the exclusion of the van der Waals radii of the surface atoms, and the channel is zigzag-like (Figures 1b,c and S1). The channel has a lining made up of alternative arrays of C−H groups and oxygen atoms, and the channel itself is chiral because of its 2-fold screw rotation symmetry. The void space is estimated 29.6% of the total volume by PLATON,[31] smaller than 33% of **3**.[16] It is apparent that the large tetrahedral nodes or the thick wall of the framework

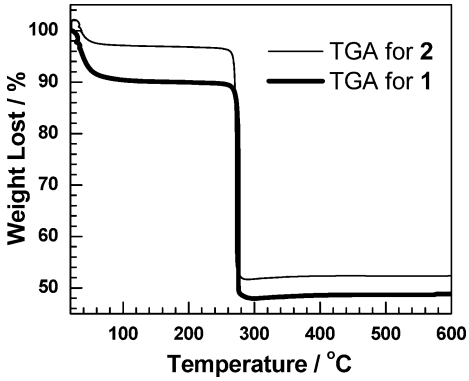


**Figure 2.** TGA runs for **1** and **2** in $N_2$ atmosphere.

prohibit the interpenetration, thus keeping the porosity of the framework, and this is, in principle we believe, the approach to build porous frameworks by using short ligands. We should note that replacement of Mn by Co in the structure resulted in a contraction of the lattice by 9%. It should also be noted that the cell volume of the manganese compound has been shown to modulate by as much as ±5% for the range of guests studied.[16] Indirectly, this is a modulation of the pores. The severe disorder of the solvent molecules lying in the channels, even at 87 K (Figure 1c), indicates a loose inclusion and possible ease of removal, which was justified by the structure determination of the desolvated compound **2** as well as other characterizations.

Compound **2** shows the same framework but with empty channels. Compound **2** has cell volume 1.1% larger than that of **1** (Table 1), together with slightly larger void space (29.9%), similar to that observed for the manganese analogue[16] and other system.[32] The expansion of the framework upon desolvation of the two compounds demonstrates the presence of the host−guest interaction, presumed through the hydrogen bonding in the parent compounds, as the framework expansion can be regarded as the loss of host−guest interactions due to the removal of small guests. Parameters of molecular geometry of the framework have minor changes in **2**, compared with that of **1** (Table 2), though showing a slight tendency of increased Co−O distances.

**Thermal Stability, Permanent Porosity, and $N_2$ Sorption of the Porous Framework.** TGA results (Figure 2) indicated that the guest molecules (methanol and water) in the framework of **1** were liberated before 100 °C. The experimental weight loss of 10.6% upon guest liberation is in agreement with the calculated value of 10.1%. The loss of the guests is also evidenced by the IR spectra of **1** and **2** (Figure S2), where the absorption bands (mainly frequencies of OH group[33]) of guests observed in **1** disappear in **2**. The framework decomposed at ca. 270 °C, similar to its Mn analogue.[16] This may be compared with the observed decomposition of the perovskite metal−formates of [AmineH$^+$]-[M(HCOO)$_3$] at 160 °C.[26] Samples of the desolvated form **2** show easy absorption of water, we presume, when exposed to air, as indicated by the weight gain (ca. 2%) at the beginning of the TGA runs, and the 3% weight loss is due to the same absorption during the period of sample preparation on the instrument. The values of weight lost for framework decomposition are within 2% of the calculated values based on $Co_2O_3$ residue. Both DTA and DSC data for **2** (Figure S3) showed only one endothermic process started at 280 °C, corresponding to the framework decomposition, and no evidence for phase transition before the framework decomposition. Therefore, the porous framework is thermally stable up to 270 °C, classifying it as a new member of porous coordination frameworks with thermal stability.

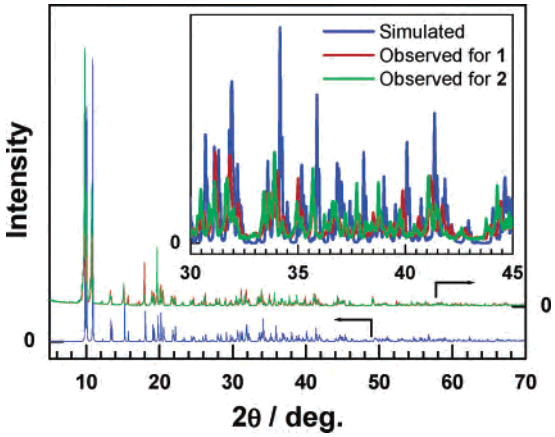


**Figure 3.** Simulated powder XRD pattern (blue) based on the structure of **1** at 87 K, and observed patterns for **1** (red) and **2** (green), both at room temperature. Inset is the detail in 2$\theta$ range 30−45°. The shift of patterns to low 2$\theta$ from the blue through red to green indicates the lattice expansion from **1** at 87 K through **1** at room temperature to **2** at room temperature.

Powder X-ray diffractions were used to check the phase of both **1** and **2**. The powder XRD pattern (Figure 3) of **2** is almost the same as that of **1**, indicating that the framework does not collapse after removal of guests. The lattice of **2** expands slightly because the powder XRD pattern of **2** shifts slightly to lower 2$\theta$ compared to **1**. All these results agree with what have been revealed by the single-crystal structure determination for **1** and **2**.

The neutron powder diffraction data (Figure S4) of the desolvated compound, **2**, were obtained at 8 and 2 K. The two temperatures, being in the paramagnetic region and the lowest temperature of the instrument D20, were used to search for magnetic scattering. We should point out that the D20 is a low-resolution instrument optimized for looking at magnetic structures and not full nuclear structures. The analysis indicates that the structure of **2** is stable to very low temperatures with a little expansion of the unit cell compared to **1**. The unit cell parameters are, at 8 K, $a$ = 11.285(3) Å, $b$ = 9.841(2) Å, $c$ = 18.141(3) Å, $\beta$ = 127.166(9)°, $V$ = 1605.4(6) Å$^3$, and at 2 K, $a$ = 11.309(3) Å, $b$ = 9.869(1) Å, $c$ = 18.201(3) Å, $\beta$ = 127.244(8)°, $V$ = 1617.3(5) Å$^3$. These results confirm the lattice expansion after removal of solvents and the permanent porosity of the material.

(31) Spek, A. L. *PLATON, A Multipurpose Crystallographic Tool*; Utrecht University: Utrecht, The Netherlands, 2001.
(32) Li, H.-L.; Eddaoudi, M.; O'Keeffe, M.; Yaghi, O. M. *Nature* **1999**, *402*, 276.
(33) Williams, D. H.; Fleming, I. *Spectroscopic Method in Organic Chemistry*, 5th ed.; McGraw-Hill Book Co.: Beijing, China, 1998.

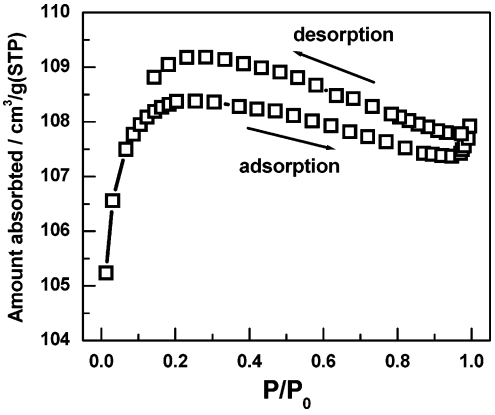


**Figure 4.** BET $N_2$ sorption isotherms at 77.4 K for **2**.

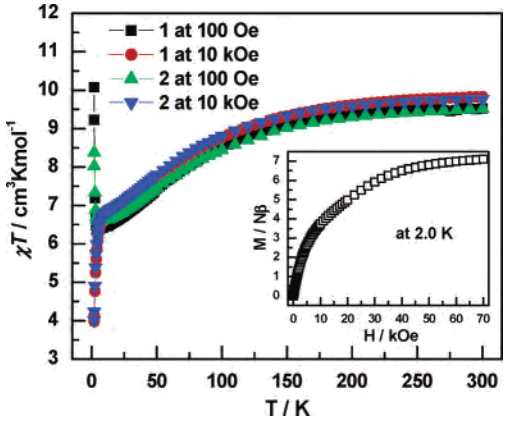


**Figure 5.** The temperature dependence of the magnetic susceptibility of **1** and **2** in applied field of 100 Oe and 10 kOe. Inset is the isothermal field dependent magnetization at 2.0 K for **1**. Magnetization at 70 kOe is 7.10 N$\beta$.

The desolvated framework **2** showed significant $N_2$ uptake (~108 mL/g when $P > 0.05$ atm, Figure 4) at 77.4 K and type I absorption behavior according to the IUPAC classification.[34] It is surprising that **2** shows such different sorption behavior on $N_2$ compared to $Mn_3(HCOO)_6$, **4**, the desolvated form of **3**, which showed no or low $N_2$ sorption, as recently reported by Kim et al.,[20] and also observed by us. It is, in fact, difficult to understand why $Mn_3(HCOO)_6$ almost did not absorb $N_2$ significantly because we have found that the $Mn_3(HCOO)_6$ framework can take up more than 40 different guests with different size, even much larger than $N_2$ and totally nonpolar solvents such as benzene and hexane.[16] Since both porous frameworks have the same structure and similar open channel, and even the pore size of the Co compound is smaller than that of Mn compound, we believe that the larger kinetic diameter of $N_2$ is not likely the reason,[20] and more detailed investigation is needed to unravel this observation. The BET surface area of **2** is 360 $m^2\ g^{-1}$, larger than that of $Mn_3(HCOO)_6$.[20] The pore volume of 0.15 $cm^3 g^{-1}$, calculated from the $N_2$ sorption data, gives the porosity of 30%, in good agreement with the estimated value of 29.9% by X-ray crystallography. That the sample of **2** after the gas adsorption experiment has a powder XRD pattern almost the same as before (Figure S5) indicates the permanent porosity and stability of the framework again.

**Magnetic Properties of 1 and 2.** Magnetic investigation on **1** and **2** revealed a tendency toward a long-range magnetic ordering at low temperature. For **1**, in a 100 Oe applied field (Figure 5), with the decrease of temperature the $\chi T$ value decreases slowly from 9.52 $cm^3$ K $mol^{-1}$ at 300 K to 8.53 $cm^3$ K $mol^{-1}$ at 100 K, and then it decreases more quickly and reaches a flat minimum of ca. 6.4 $cm^3$ K $mol^{-1}$ between 20 and 4 K. After that, the $\chi T$ value rises sharply to 10.08 $cm^3$ K $mol^{-1}$ at 1.9 K, indicating enhanced magnetism toward long-range magnetic ordering. ac susceptibility measurements in zero dc field (Figure S6) for **1** also indicate the presence of a possible magnetic transition below 2.5 K. The dc data above 50 K can be fitted to the Curie−Weiss law with $C =$ 10.22 $cm^3$ K $mol^{-1}$ and $\theta = -19.4$ K. The decrease of $\chi T$ from room temperature to low temperature is due principally to the effect of spin−orbit coupling of the Co(II) ion, which results in an effective $S = {}^1/_2$ at low temperature from an $S = {}^3/_2$ at high temperature due to the depopulation of the higher energy Kramers doublets ($\pm{}^3/_2$ and $\pm{}^5/_2$).[35] This is equivalent to the $\theta$ value of ca. −20 K. In a 10 kOe field, $\chi T$ behaves similarly above 8 K; however, it goes down sharply below 8 K to 3.98 $cm^3$ K $mol^{-1}$ at 1.9 K. This indicates that the long-range magnetic ordering might be antiferromagnetic with spin-canting,[36] but more detailed study is needed to understand it. The $M$ versus $H$ plot (Figure 5, inset) at 2.0 K confirms that the transition has not been reached, and the magnetization at 70 kOe is 7.10 $N\beta$, close to that expected for three cobalt atoms.[35] The temperature dependence of the magnetic susceptibility of **2** is almost the same as that of **1**. Furthermore, on the powder neutron diffraction data of **2** there is no magnetic scattering observed at 2 K, suggesting that the rise in magnetization near 2 K may be associated with enhancement of the short-range correlation. The magnetic investigation at lower temperature below 2 K, which is not reachable by instruments we used, would be needed to reveal the nature of the magnetic ordering.

## Conclusion

In summary, we have prepared a diamond framework with Co-centered $CoCo_4$ tetrahedral nodes and open channels. The framework is the first example of Co−formates without co-ligands. It displays permanent porosity, thermal stability up to 270 °C, and probable 3D long-range magnetic ordering at low temperature. The result demonstrates that the simple and short ligands are beneficial for the formation of nanoporous magnetic coordination frameworks with thick walls that prevent interpenetration. Since the material shows the similar structure and stability to the Mn analogue, the

(34) IUPAC. *Pure Appl. Chem.* **1985**, *57*, 603.

(35) (a) Carlin, R. L. *Magnetochemistry*; Springer-Verlag: Berlin, 1986; pp 65−67. (b) Figgis, B. N.; Lewis, J. *Prog. Inorg. Chem.* **1964**, 37. (c) Figgis, B. N.; Gerloch, M.; Lewis, J.; Mabbs, F. E.; Webb, G. A. *J. Chem. Soc. A* **1968**, 2086. (d) Palii, A. V.; Tsukerblat, B. S.; Coronado, E.; Clemente-Juan, J. M.; Borras-Almenar, J. J. *Inorg. Chem.* **2003**, *42*, 2455.

(36) Banister, A. J.; Bricklebank, N.; Lavender, I.; Rawson, J. M.; Gregory, C. I.; Tanner, B. K.; Clegg, W.; Elsegood, M. R. J.; Palacio, F. *Angew. Chem., Int. Ed. Engl.* **1996**, *35*, 2533.

material will be expected to display a wide range of guest inclusion behavior, and thus provides a new case for the study of interaction between the porous magnetic framework and guests in both magnetism and structural respects. The achievement of both isomorphs (and other members of this family[21]) reveals the possibility to obtain the mixed metal porous frameworks with controllable pore size and different magnetic behavior and therefore may provide new porous materials showing guest-modulated magnetic properties.

**Acknowledgment.** Z.W. would like to acknowledge the financial support of the National Science Foundation of China (90201014 and 20491101), and Prof. Song Gao and Mr. Haoling Sun of the College of Chemistry and Molecular Engineering, Peking University, for their kind help with magnetic measurements.

**Supporting Information Available:** X-ray crystallographic file in CIF format of compounds **1** (87 and 180 K) and **2** (105 and 180 K), and a PDF file containing additional figures (Figure S1−S6). This material is available free of charge via the Internet at http://pubs.acs.org.

IC048986R